JACS JOURNAL OF THE AMERICAN CHEMICAL SOCIETY

COMMUNICATION

pubs.acs.org/JACS

Chiral Nematic Assemblies of Silver Nanoparticles in Mesoporous Silica Thin Films

Hao Qi,[†] Kevin E. Shopsowitz,[†] Wadood Y. Hamad,[‡] and Mark J. MacLachlan[*,†]

[†]Department of Chemistry, University of British Columbia, 2036 Main Mall, Vancouver, BC, Canada V6T 1Z1

[‡]FPInnovations, 3800 Wesbrook Mall, Vancouver, BC, Canada V6S 2L9

S *Supporting Information*

ABSTRACT: Silver nanoparticles (NPs) have been synthesized inside mesoporous silica films with chiral nematic structure. Circular dichroism measurements of the silver NP-loaded silica films show NP-based optical activity in the vicinity of the surface plasmon resonance. These materials, with an optical response associated with the chiral assembly of metal NPs, may be useful for developing new sensors.

Metal nanoparticles (NPs) represent an important class of building blocks for constructing new functional materials such as catalysts and sensors.[1] By capping NPs with a selection of ligands, the optical and other properties of the structures can be modified.[2] On the other hand, controlling the supramolecular organization of the NPs can introduce additional functionality.[3]

An important and interesting property of some metal NPs is chirality. Despite a considerable amount of work in this area, the origin of the observed optical activity (usually by circular dichroism, CD) in the surface plasmon resonance (SPR) of metal NPs is still debated.[4] Whetten, whose pioneering work gave the first example of chiral ligand-protected Au NPs,[5] proposed three possible mechanisms (chiral core, chiral surface, and chiral organization) that have been extensively studied to explain the origin of chirality.[6,7] The vast majority of NPs that show optical activity have been prepared with small chiral capping molecules.

To study the chirality of NPs, several researchers have turned to biological scaffolds. Shemer et al. used DNA to template the synthesis of Ag NPs.[6h] The intrinsic chiral core of the NPs has been discussed as the probable origin of the chirality, but the authors also proposed the possible contribution of the helical structure of DNA. In another paper, Thomas used peptide nanotubes as a scaffold to synthesize Au NPs and observed a signal by CD.[6i] In that case the chiral organization of Au NPs was regarded as the source of the observed CD signal, but the authors clearly mentioned that they cannot rule out the possibility of individual chiral NPs. Prasad and co-workers very recently showed a plasmonic enhancement of the optical activity of chiral poly(fluorene-*alt*-benzothiadiazole) doped with Au NPs and proposed a combination of enhancement mechanisms dominated by helical ordering of Au NPs.[8] These reports indicate that, regardless of the chirality of the individual NPs, the chiral assembly of metal NPs might be another important aspect of the chiral response of NPs. Chirality transfer from chiral host materials such as polymers or liquid crystals to achiral organic dopants (e.g., a dye) is well known.[9] If NPs are used in place of a dye, the same type of chirality transfer may also occur.

Chiral assemblies of NPs or chiral nanostructures have been extensively studied and visualized by techniques such as electron microscopy and atomic force microscopy.[10] As one example, Rosi assembled Au NPs into double helices with the help of a peptide template.[10c] These studies raise an intriguing question: can all of these chiral assemblies of metal NPs give related chiral optical activities that are measurable by CD? Recent theoretical calculations indicate that NPs organized into a helical structure should show large CD signals in the visible spectrum due to Coulombic interactions between NPs in the assembly.[11]

By using nanocrystalline cellulose (NCC) as template, we recently reported the first mesoporous silica films with chiral nematic ordering.[12] The helical pitch in the mesoporous silica is easily tuned by changing the ratio of the silica precursor relative to NCC, thus varying the wavelength of reflected light from the UV to the near IR. In this report, we used the chiral mesoporous silica films as hosts to organize Ag NPs. Observed CD signals for the Ag NPs synthesized in situ derive from supramolecular organization of the NPs rather than from chirality of the individual NPs that might be transferred from the chiral NCC template.

Colorless mesoporous silica films with reflection peaks above 1000 nm were used so that the reflection does not overlap with the SPR peak of Ag NPs (390−420 nm).[13] Two chiral silica samples (**Si1** and **Si2**) were prepared, with reflection peaks around 1050 and 1450 nm, respectively (Figure 1a). Chiral nematic ordering of the films can be clearly seen from scanning electron microscopy (SEM) images (Figure 1c,d and Figure S1, S2). The Brunauer−Emmett−Teller surface areas of **Si1** and **Si2** are 769 and 470 m^2/g, respectively.

CD measurements of small pieces of **Si1** and **Si2** show small signals between 300 and 800 nm that are artifacts owing to birefringence (Figure 1b).[14] When the pores are filled with water, a change in refractive index alters the intensity of the birefringence, but the overall shapes of the spectra hardly change.

To prepare Ag NPs within the mesoporous silica, the films were first soaked in $AgNO_3$ solutions for 30 min, removed from the solution, and rinsed with de-ionized water and acetone to remove surface-bound Ag^+. After drying in air, the films were soaked in freshly prepared 200 mM $NaBH_4$ solution to reduce the Ag^+ to Ag^0 and form Ag NPs in the pores. Based on the silica

Received: November 18, 2010
Published: February 28, 2011

dx.doi.org/10.1021/ja110369d | *J. Am. Chem. Soc.* 2011, 133, 3728–3731

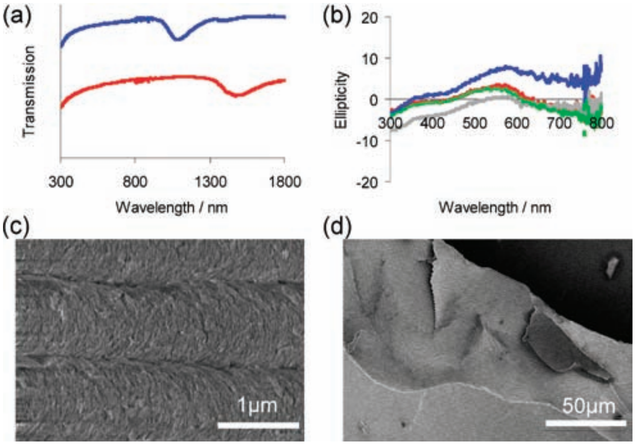

Figure 1. (a) UV−vis transmission spectra of **Si1** (blue) and **Si2** (red). (b) CD spectra of **Si1** (blue), **Si1** soaked with water (green), **Si2** (red), and **Si2** soaked with water (gray). (c,d) SEM images of **Si1** at different magnifications.

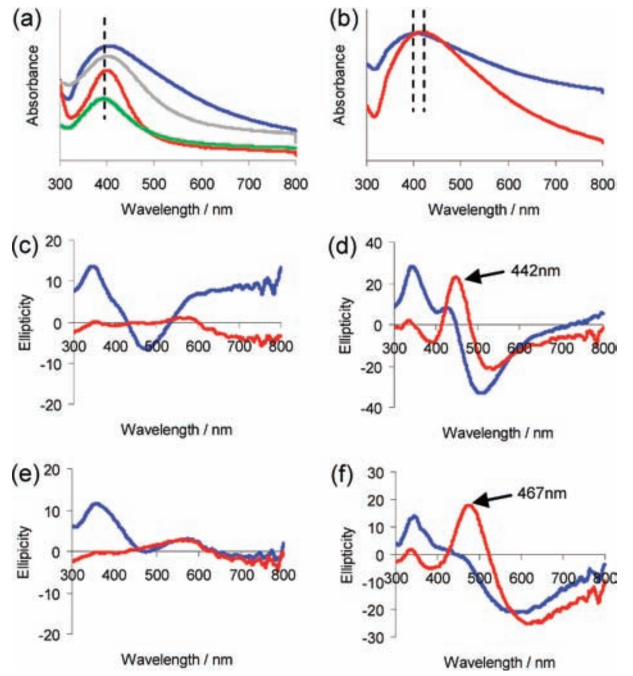

Figure 2. (a) UV−vis spectra of Ag NP samples: **Ag1-a** (green), **Ag1-b** (gray), **Ag2-a** (red), **Ag2-b** (blue). (b) UV−vis spectra of **Ag2-b** before (blue) and after (red) soaking with water. (c−f) CD spectra of Ag NPs loaded silica film before (blue) and after (red) soaking with water: (c) **Ag1-a**, (d) **Ag1-b**, (e) **Ag2-a**, (f) **Ag2-b**.

samples (**Si1** and **Si2**) and the different $AgNO_3$ concentrations being used ((**a**) 10 mM and (**b**) 100 mM), four different samples were prepared, namely **Ag1-a**, **Ag1-b**, **Ag2-a**, and **Ag2-b**. Compared to the colorless and transparent pure silica films **Si1** and **Si2**, films loaded with Ag NPs have transparent light yellow (**Ag1-a**, **Ag2-a**) or dark yellow (**Ag1-b**, **Ag2-b**) colors.

The UV−vis absorption spectra of films loaded with Ag NPs show a peak near 400 nm assigned to the SPR (Figure 2a). The SPR absorption peaks are slightly shifted when the pores are filled with water (Figure 2b). CD spectra of the samples containing Ag NPs are shown in Figure 2c−f. Compared with the CD spectra of the pure silica samples (Figure 1b), where only small artifact signals are observed, CD spectra of the NP-loaded samples show much stronger signals. Samples were rotated perpendicular to the light beam to eliminate the possibility that the CD signals arose only from linear dichroism (Figure S3).[14] Although films of similar sizes were used for all measurements, quantitative comparison of the CD signal intensities between the different samples is not possible since the brittleness of the films did not allow films of the exact same size to be used.

Compared to the UV−vis spectra, the CD spectra of wet and dry Ag NP samples differ dramatically. For **Ag1-a** and **Ag2-a**, which were prepared using a 10 mM (low concentration) $AgNO_3$ solution, the intensities of the signals in the CD spectrum are greatly reduced when the pores are filled with water (Figure 2c,e). In contrast, when the pores of **Ag1-b** and **Ag2-b** (prepared with 100 mM $AgNO_3$ solution) are filled with water, the intensities and the overall shapes of the CD spectra change (Figure 2d,f).

The SPR of metal NPs is sensitive to the size and ordering of the NPs (e.g., space between NPs or NP assemblies), as well as to the dielectric properties of the surrounding media, which is the basis for using metal NPs for biosensors.[15] The similar SPR peaks (Figure 2a) for the different Ag NP samples we examined indicate that the sizes of the Ag NPs are all similar, perhaps restricted by the pore size in the materials. Samples prepared with a higher concentration of Ag^+ have more Ag NPs within the pores, thus reducing the distance between the NPs. This is the main difference between **Ag1-a** and **Ag1-b** as well as between **Ag2-a** and **Ag2-b**. As the dielectric property of the medium surrounding the NPs changes upon filling with water, the SPR of the NPs will change (Figure 2b).[15a] Consequently, changes are observed in the SPR band in the absorbance-based CD spectra. The large changes observed in the CD spectra upon filling the pores with water mean that the optical activity is more sensitive than the positions of the SPR absorbance peaks to changes in the environment, thus opening up a unique approach for biosensing-related applications.

During templation of the mesoporous silica with NCC, chirality may possibly be transferred to the silica at three different length scales: (i) from the molecular level, since the NCC is composed of chiral D-glucose units, (ii) from the screw-shaped morphology of individual nanocrystals,[16] and (iii) from the long-range chiral nematic ordering of the NCC. The chiral nematic structure of the silica films has been proven,[12] but we do not know whether the other levels of chirality are transferred to the silica (and possibly affect the chirality of the individual NPs). Thus, we sought experimental support that the chiral signal observed by CD originates from long-range organization of the NPs in the chiral nematic host rather than from the chirality of the individual NPs or NP assembies within single pores.

Ag1-b and **Ag2-b**, which differ in the pitch of the chiral nematic template, show completely different responses by CD upon filling the samples with water (Figure 2d,f). As **Si-1** and **Si-2** are both templated from NCC and have chiral nematic ordering, the individual pore structures should be very similar. Indeed, both have similar N_2 adsorption/desorption isotherms and BJH pore size distributions (Figure S4). Thus, the main differences between **Si-1** and **Si-2** are the helical pitch and silica wall thickness. Furthermore, **Ag1-b** and **Ag2-b** were prepared using the same concentration of $AgNO_3$. Therefore, the different CD response of the two Ag NP samples must stem from the overall different helical pitch and wall thickness rather than differences between individual NPs or the NP assemblies within single pores.

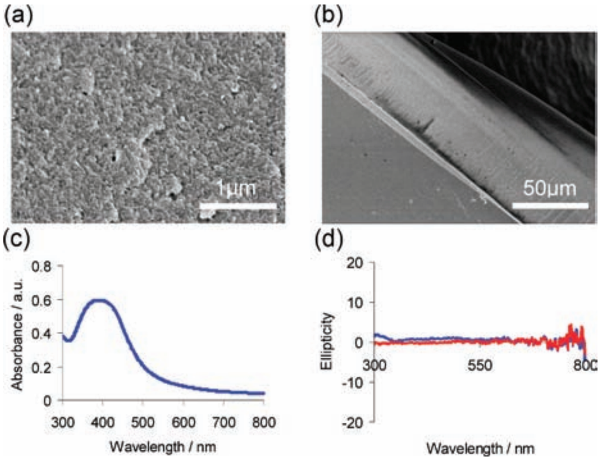

Figure 3. (a,b) SEM images of **Si3** film without chiral nematic ordering at different magnifications . (c) UV−vis spectrum of **Ag3**. (d) CD spectra of **Ag3** before (blue) and after (red) soaking with water.

The fact that the helical pitch of the silica films affects the CD signal of the Ag NPs gives evidence that the observed optical activity is due to a long-range chiral nematic organization.

To further prove that the optical activity is due to the organization of the Ag NPs within the chiral nematic host, we prepared a new mesoporous silica using NCC as template, but without chiral nematic ordering. In our previous study, we found that slightly changing the pH can nullify the chiral nematic ordering of NCC/silica composite films as well as calcined mesoporous silica films.[12] Thus, sample **Si3** was prepared using NCC as a template at pH 2. SEM images of as-prepared **Si3** silica films did not reveal any ordering (Figure 3a,b and Figure S5). UV−vis and CD spectra also did not show any signal originating from chirality in the sample (Figure S6). However, the N_2 gas adsorption/desorption isotherms and BJH pore size distributions for **Si3** are quite similar to those of **Si1** and **Si2** (Figure S7), confirming that the pores are formed around individual NCC crystallites. **Si3** was loaded with Ag NPs using the same procedure as described above (100 mM $AgNO_3$). Silica films loaded with Ag NPs (namely **Ag3**) without chiral nematic ordering show similar positions of the SPR peak in the UV−vis spectrum to the chiral nematic samples, suggesting that the Ag NPs have similar sizes as in **Ag1** and **Ag2** (Figure 3c). CD measurement of **Ag3** showed no related CD signals. Moreover, the films did not show any change in optical activity upon filling with water (Figure 3d). These results also support the conclusion that the CD signals observed for **Ag1** and **Ag2** originate from the long-range chiral nematic order in those samples.

Sample **Ag1-b** was also characterized by transmission electron microscopy (TEM) (Figure S8). Nanosized Ag particles can be clearly observed, along with the somewhat twisted one-dimensional silica pores. As we had to grind the film and use the powder dispersed in ethanol for the TEM sample, it is more difficult to see any evidence for chiral nematic ordering and the process inevitably causes the release of some NPs from the pores. Also, since the chiral nematic organization has a pitch of over 1000 nm in these samples, we did not expect to be able to visualize the chiral nematic structure by TEM.

The NPs were further isolated by capping them with hexanethiol and dissolving the silica with $NaOH_{(aq)}$. TEM measurements show Ag NPs with sizes around 3−5 nm, which matches closely the pore diameter of the silica host (Figure S9). UV−vis spectra show a slope at 300−800 nm without an obvious SPR peak (Figure S10). Comparing the UV−vis spectrum of the free Ag NPs in solution to those loaded in silica films, the strong SPR peaks of Ag NP-loaded silica films may indicate an assembling behavior that gives rise to strong electronic interactions between the NPs. It is also likely that the NPs are etched by the thiols and change size accordingly.[17] CD measurement of NP solutions did not show a signal, meaning there is no optical activity associated with the released NPs (Figure S10b).

In conclusion, we have demonstrated that Ag NPs can be formed inside chiral nematic mesoporous silica films. CD measurement of these silica films loaded with Ag NPs showed optical activities in the vicinity of the SPR of the Ag NPs. Based on the comparison of CD spectra of **Ag1-b** and **Ag2-b**, as well as the result of **Ag3**, we believe the optical activities solely originate from the long-range organization of the Ag NPs in the chiral nematic silica host. We believe this is a clear example of a truly chiral assembly of metal nanoparticles with related optical activity where the optical activity definitively originates from the chiral organization rather than from a property of the individual NPs. It is likely that other chiral assemblies of NPs, such as those assembled on biological structures, will also exhibit optical activity. Considering the importance of using SPR of metal NPs for biosensing applications, using the response based on the chiral organization of metal NPs embedded in a chiral mesoporous host will certainly open up new directions for related applications.

■ ASSOCIATED CONTENT

Ⓢ **Supporting Information.** Details of synthesis procedures and characterization, larger images of UV−vis and CD spectra, and supplementary SEM and TEM images. This information is available free of charge via the Internet at http://pubs.acs.org.

■ AUTHOR INFORMATION

Corresponding Author

mmaclach@chem.ubc.ca

■ ACKNOWLEDGMENT

We thank NSERC and FPInnovations for support.

■ REFERENCES

(1) Daniel, M.-C.; Astruc, D. *Chem. Rev.* **2004**, *104*, 293–346.

(2) (a) Burda, C.; Chen, X.; Narayanan, R.; El-Sayed, M. A. *Chem. Rev.* **2005**, *105*, 1025–1102. (b) Xia, Y.; Yang, P.; Sun, Y.; Wu, Y.; Mayers, B.; Gates, B.; Yin, Y.; Kim, F.; Yan, H. *Adv. Mater.* **2003**, *15*, 353–389. (c) Sastry, M.; Rao, M.; Ganesh, K. N. *Acc. Chem. Res.* **2002**, *35*, 847–855.

(3) (a) Nie, Z. H.; Petukhova, A.; Kumacheva, E. *Nat. Nanotech.* **2010**, *5*, 15–25 and references therein. (b) Kotov, N. A.; Stellacci, F. *Adv. Mater.* **2008**, *20*, 4221–4222. (c) Chen, C. L.; Rosi, N. L. *Angew. Chem., Int. Ed.* **2010**, *49*, 1924–1942.

(4) (a) Noguez, C.; Garzón, I. L. *Chem. Soc. Rev.* **2009**, *38*, 757–771. (b) Gautier, C.; Bürgi, T. *ChemPhysChem* **2009**, *10*, 483–492. (c) Kitaev, V. *J. Mater. Chem.* **2008**, *18*, 4745–4749.

(5) Schaaff, T. G.; Whetten, R. L. *J. Phys. Chem. B* **2000**, *104*, 2630–2641.

(6) (a) Gautier, C.; Bürgi, T. *J. Am. Chem. Soc.* **2006**, *128*, 11079–11087. (b) Gautier, C.; Bürgi, T. *J. Am. Chem. Soc.* **2008**, *130*, 7077–7084. (c) Si, S.; Gautier, C.; Boudon, J.; Taras, R.; Gladiali, S.;

Bürgi, T. *J. Phys. Chem. C* **2009**, *113*, 12966–12969. (d) Yao, H.; Miki, K.; Nishida, N.; Sasaki, A.; Kimura, K. *J. Am. Chem. Soc.* **2005**, *127*, 15536–15543. (e) Yao, H.; Fukui, T.; Kimura, K. *J. Phys. Chem. C* **2007**, *111*, 14968–14976. (f) Cathcart, N.; Mistry, P.; Makra, C.; Pietrobon, B.; Coombs, N.; Jelokhani-Niaraki, M.; Kitaev, V. *Langmuir* **2009**, *25*, 5840–5846. (g) Qi, H.; Hegmann, T. *J. Am. Chem. Soc.* **2008**, *130*, 14201–14206. (h) Shemer, G.; Krichevski, O.; Markovich, G.; Molotsky, T.; Lubitz, I.; Kotlyar, A. B. *J. Am. Chem. Soc.* **2006**, *128*, 11006–11007. (i) George, J.; Thomas, K. G. *J. Am. Chem. Soc.* **2010**, *132*, 2502–2503.

(7) (a) Román-Velázquez, C. E.; Noguez, C.; Garzón, I. L. *J. Phys. Chem. B* **2003**, *107*, 12035–12038. (b) Goldsmith, M.-R.; George, C. B.; Zuber, G.; Naaman, R.; Waldeck, D. H.; Wipf, P.; Beratan, D. N. *Phys. Chem. Chem. Phys.* **2006**, *8*, 63–67. (c) Sánchez-Castillo, A.; Noguez, C.; Garzón, I. L. *J. Am. Chem. Soc.* **2010**, *132*, 1504–1505.

(8) Oh, H. S.; Liu, S.; Jee, H.; Baev, A.; Swihart, W. T.; Prasad, P. N. *J. Am. Chem. Soc.* **2010**, *132*, 17346–17348.

(9) (a) Palmans, A. R. A.; Meijer, E. W. *Angew. Chem., Int. Ed.* **2007**, *46*, 8948–8968. (b) Goodby, J. W.; Saez, I. M.; Cowling, S. J.; Görtz, V.; Draper, M.; Hall, A. W.; Sia, S.; Cosquer, G.; Lee, S.-E.; Raynes, E. P. *Angew. Chem., Int. Ed.* **2008**, *47*, 2754–2787.

(10) (a) Bierman, M. J.; Lau, Y. K. A.; Kvit, A. V.; Schmitt, A. L.; Jin, S. *Science* **2008**, *320*, 1060–1063. (b) Morin, S. A.; Bierman, M. J.; Tong, J.; Jin, S. *Science* **2010**, *328*, 476–480. (c) Chen, C.-L.; Zhang, P.; Rosi, N. L. *J. Am. Chem. Soc.* **2008**, *130*, 13555–13557. (d) Chen, C.-L.; Rosi, N. L. *J. Am. Chem. Soc.* **2010**, *132*, 6902–6903. (e) Sharma, J.; Chhabra, R.; Cheng, A.; Brownell, J.; Liu, Y.; Yan, H. *Science* **2009**, *323*, 112–116.

(11) Fan, Z.; Govorov, A. O. *Nano Lett.* **2010**, *10*, 2580–2587.

(12) Shopsowitz, K. E.; Qi, H.; Hamad, W. Y.; MacLachlan, M. J. *Nature* **2010**, *468*, 422–425.

(13) Cao, Y. W.; Jin, R. C.; Mirkin, C. A. *J. Am. Chem. Soc.* **2001**, *123*, 7961–7962.

(14) Spitz, C.; Dähne, S.; Ouart, A.; Abraham, H.-W. *J. Phys. Chem. B* **2000**, *104*, 8664–8669.

(15) (a) Liz-Marzán, L. M. *Langmuir* **2006**, *22*, 32–41. (b) Rosi, N. L.; Mirkin, C. A. *Chem. Rev.* **2005**, *105*, 1547–1562.

(16) Habibi, Y.; Lucia, L. A.; Rojas, O. J. *Chem. Rev.* **2010**, *110*, 3479–3500 and references therein.

(17) Schaaff, T. G.; Whetten, R. L. *J. Phys. Chem.* **1999**, *103*, 9394–9396.